[Review Paper]

Noble Metal Phosphides as New Hydrotreating Catalysts: Highly Active Rhodium Phosphide Catalyst

Yasuharu KANDA* and Yoshio UEMICHI

Applied Chemistry Research Unit, College of Environmental Technology, Graduate School of Engineering, Muroran Institute of Technology, 27-1 Mizumoto, Muroran, Hokkaido 050-8585, JAPAN

(Received August 1, 2014)

Metal phosphide has been widely investigated as a hydrotreating catalyst. The preparation and performance of noble metal phosphide catalyst was examined to develop new phosphide hydrotreating catalysts. The supports affect reducibility of phosphate as a P precursor. Since phosphate does not strongly interact with SiO_2 and TiO_2 supports, Rh_2P was easily formed on these supports. Furthermore, formation of Rh_2P enhanced the hydrodesulfurization (HDS) activity of supported Rh–P catalyst. The type of noble metal (NM) and P/NM ratio also strongly affect formation of noble metal phosphide and HDS activity. Excess P facilitates formation of noble metal phosphides at lower reduction temperature. In contrast, excess P causes the aggregation of noble metal phosphide and formation of phosphorus rich noble metal phosphide. Rh–1.5P/SiO_2 catalyst had high and stable activity for HDS reaction. Furthermore, this catalyst showed significantly higher hydrodenitrogenation (HDN) activity than sulfided NiMoP/Al_2O_3 catalyst. Therefore, Rh_2P has great potential as a new hydrotreating catalyst.

Keywords

Noble metal phosphide, Hydrotreating catalyst, Hydrodesulfurization, Hydrodenitrogenation

1. Introduction

Substantial efforts are being made worldwide to develop technologies for solving environmental problems. Sulfur oxides (SO_x), which are formed by the combustion of organic sulfur compounds in fuels, cause air pollution, acid rain and deactivation of automotive exhaust catalysts. Consequently, clean fuels have been produced in the petroleum industry using hydrodesulfurization (HDS) processes based on sulfided Co(Ni)Mo/Al_2O_3 catalysts. Heavy oil contain greater quantities of sulfur compounds compared with gasoline and diesel fuel, so regulation of SO_x emissions from ships is expected to become more stringent. Recently, the petroleum industry claimed that the development of highly active HDS catalysts with higher activity than commercial CoMo catalysts will prevent environmental problems and the deactivation of automotive exhaust catalysts[1)~4)].

The Co–Mo–S phase is the active site of sulfided CoMo/Al_2O_3 catalyst[1),4),5)]. Various methods for preparing highly active CoMo-based HDS catalysts, such as the Co chemical vapor deposition (CVD) technique[1),4)], and addition of phosphorus[1),6),7)] and chelating agents[1),8),9)], have been widely investigated to form the Co–Mo–S phase. Furthermore, new phases active as new HDS catalysts, such as carbides[10)~14)], nitrides[10),11),15)], and phosphides[2),3),14),16)~38)], have been reported. In particular, transition metal phosphides, such as Ni_2P[2),3),14),16)~34)] and MoP[18),19),36)~40)], have received extensive attention[2),3),34)].

Hydrogenation is an important method for the desulfurization of refractory organic sulfur compounds, such as 4,6-dimethyldibenzothiophene[4),29),41)]. Furthermore, since organic nitrogen compounds are well known to poison HDS catalyst[42)~45)], any high performance HDS catalyst should have high hydrodenitrogenation (HDN) activity. HDN of aromatic nitrogen compound occurs through hydrogenation of the aromatic ring, followed by cleavage of the C–N bond to form NH_3 and hydrocarbon[28),45),46)]. Therefore, high hydrogenation activity is one of the important characteristics of highly active HDS catalyst.

Recently, we reported that noble metal (NM), especially Pt, catalysts showed high and stable HDS activities[47)~53)]. We proposed two reaction mechanisms for the HDS reaction: the monofunctional route occurring on Pt particles, and the bifunctional route occurring on Pt and Brønsted acid sites[47)~53)]. Therefore, noble metal phosphide catalyst, which has moderate hydrogenation activity, can be expected to show high HDS and HDN activities.

DOI: dx.doi.org/10.1627/jpi.58.20

* To whom correspondence should be addressed.

* E-mail: kanda@mmm.muroran-it.ac.jp

This review introduces the effects of reduction temperature, support, and P/NM ratio on the formation of noble metal phosphides as new HDS catalysts and describes their HDS and HDN activities[54)~58)].

2. Effect of Supports on Formation of Noble Metal Phosphides and Hydrodesulfurization Activities

2. 1. Synthesis of Bulk Metal Phosphides

Numerous synthesis methods, such as combination of elements, solid state metathesis, reaction with phosphine, decomposition of organometallics, electrolysis of salts, and reduction of phosphate, have been reported for the preparation of metal phosphides[3),19)]. Among these methods, phosphate reduction is a convenient and simple method to prepare phosphide catalysts[19)]. Tungsten phosphide (WP) was synthesized by the reduction of tungsten phosphate, which was prepared from evaporation of ammonium metatungstate and ammonium phosphate aqueous solution[35)]. Other phosphides (Ni_2P and MoP) have also been prepared by phosphate reduction[26),28),30)]. $NH_4NiPO_4 \cdot nH_2O$ reduced with hydrogen (5 vol%, at 650-750 ℃) reacts to form Ni_2P[20)]. Rh_2P and Ir_2P were also synthesized by phosphate reduction[59)]. Rh_2P as a single crystalline phase was formed after reduction at 375 ℃[59)]. In contrast, Ir_2P was formed after reduction at 600 ℃, but metallic Ir was also present as an impurity[59)].

2. 2. Effect of Supports on Formation of Ni_2P and Hydrodesulfurization Activity

The support is known to affect the HDS activity of Ni_2P catalyst. H_3PO_4 probably reacts with Al_2O_3 and SiO_2–Al_2O_3 to form $AlPO_4$, rather than reacts with Ni to form Ni_2P[16)]. XPS analysis revealed that $AlPO_4$ was formed in Ni_2P/Al_2O_3 catalysts, whereas silicon phosphates did not occur in Ni_2P/SiO_2 catalysts[24)]. These findings indicate that SiO_2 does not strongly interact with phosphate. Therefore, SiO_2 is a suitable support for Ni_2P catalyst.

TiO_2 has been widely investigated as a support for hydrotreating catalysts[4),40),41),60)~63)]. Ni_2P catalyst can be prepared on TiO_2, as well as SiO_2 support[64)]. Addition of TiO_2 enhances the C–N bond cleavage activity of MoP/MCM-41 catalyst, but inhibits the dehydrogenation activity[40)]. The support affects the HDS activity of CoMo catalysts[45)] and the acidity of the support enhances the sulfur tolerance of noble metal-based HDS catalysts[65)~67)]. Consequently, the support may have important effects on the formation and HDS activity of Rh_2P, which is more easily formed than Ni_2P and Ir_2P.

2. 3. Formation of Rh_2P on Various Metal Oxide Supports[55)]

Reduction temperature is one of the important factors in the reducibility of phosphate and the formation of phosphide. **Figure 1** shows the temperature programmed reduction (TPR) profiles of 1.5 wt% P-added Rh (Rh–1.5P, 5 wt% Rh, P/Rh molar ratio = 1.0) catalyst supported on various metal oxides (MO_x). Rh_2O_3 reduction (from 50 to 150 ℃) showed peaks for all Rh–1.5P/MO_x catalysts, except on MgO support. Moreover, reduction peaks for all phosphates occurred above 150 ℃. Broad peaks appeared at 270, 360 and 650 ℃ for the Rh–1.5P/SiO_2 catalyst. We reported that H_2 consumption appeared above 700 ℃ in the TPR profile of P/SiO_2 catalyst[57)]. Furthermore, two peaks at approximately 50 ℃ and above 650 ℃ occurred for the physically mixed Rh/SiO_2 and P/SiO_2 catalysts, in which the Rh_2O_3 hardly interacted with the phosphate[58)]. Therefore, the reduction peak in the range of 200-350 ℃ was attributed to reduction of the phosphate that interacted with the Rh_2O_3. Reduction peaks were observed at 280, 540 and 730 ℃, and a shoulder peak appeared at 400 ℃ for the Rh–1.5P/TiO_2 catalyst. TiO_2 is well known to be more reducible than other metal oxides[68),69)]. Therefore, the large peak observed at 540 ℃ would include reduction of the TiO_2 support. The profile of Rh–1.5P/Al_2O_3 catalyst showed no reduction peaks from 200 to 600 ℃, but H_2 consumption increased above 700 ℃. Phosphate reacts with the surface of Al_2O_3 to form $AlPO_4$ in the Ni_2P/Al_2O_3 catalyst[16),24)]. Therefore, the H_2 consumption observed above 700 ℃ was attributed to the reduction of $AlPO_4$. The same trend was also observed in the TPR profile of Rh–1.5P/ZrO_2, indicating the presence of zirconium phosphate. On the other hand, the reduction peak of $MgRh_2O_4$[70)] appeared at 550 ℃ in the TPR profile of Rh–P/MgO catalyst. Furthermore, X-ray diffraction (XRD) showed no peaks for Rh species in calcined Rh–1.5P/MgO catalyst, implying that highly dispersed $MgRh_2O_4$ is present in the Rh–1.5P/MgO catalyst.

The XRD peak intensities of metallic Rh ($2\theta = 40.9°$) and Rh_2P ($2\theta = 46.7°$) in reduced Rh–1.5P/MO_x catalysts are also shown in **Fig. 1**. The intensity of metallic Rh decreased with higher reduction temperature, whereas the intensity of Rh_2P increased, in all catalysts. Furthermore, remarkable increase in Rh_2P intensity agreed with observed phosphate reduction (TPR profile). On the basis of these findings, the order of formation temperature of Rh_2P on MO_x support was SiO_2–TiO_2 < MgO < ZrO_2 < Al_2O_3.

2. 4. Hydrodesulfurization Activities of Metal Oxide-supported Rh_2P Catalysts[55)]

The type of support strongly affects Rh_2P formation, as shown in **Fig. 1**. Therefore, we evaluated the HDS activities of Rh–1.5P/MO_x catalysts reduced at various temperatures[56)]. **Table 1** shows the catalytic activities of Rh–1.5P/MO_x for the HDS of thiophene (C_4H_4S). The optimal reduction temperature for the highest activity remarkably changed with the type of MO_x support. The highest activity appeared at low reduction temperature (550 ℃) for Rh–1.5P/SiO_2 catalyst, whereas

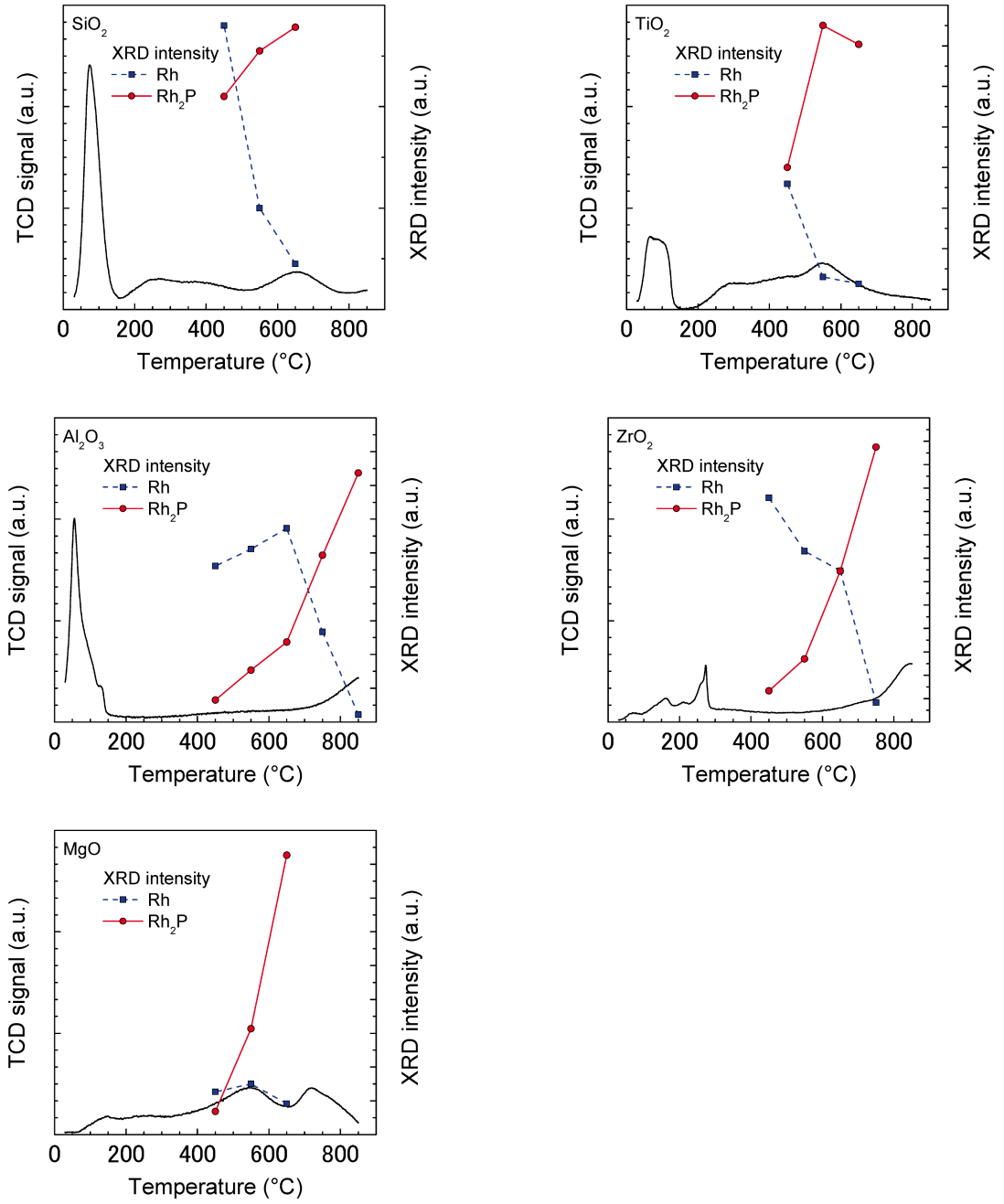

Intensities of Rh and Rh_2P peaks were measured at $2\theta = 40.9°$ and 46.7°, respectively.

Fig. 1 TPR Profiles of Rh–1.5P/MO_x Catalysts[56] and Intensities for Rh and Rh_2P Peaks Observed in XRD Patterns of the Rh–P/MO_x Catalysts after Reduction at Various Temperatures

the highest HDS activities occurred at higher reduction temperatures (above 650 ℃) for other supports. These findings suggest that the formation temperature of Rh_2P significantly depends on the type of MO_x support. Regardless of the relatively easy formation of Rh_2P, the highest HDS activity for Rh–1.5P/TiO_2 catalyst was obtained at 650 ℃. The order of HDS activities was SiO_2–TiO_2–Al_2O_3 > MgO > ZrO_2.

Table 1 also shows the TOFs of Rh–1.5P/MO_x catalysts calculated from the CO uptake (assuming CO/Rh = 1). The TOFs of Rh–1.5P catalysts were remarkably enhanced by Rh_2P formation. The order of TOFs for Rh–1.5P catalysts was TiO_2 > ZrO_2 > Al_2O_3 > SiO_2 > MgO. TiO_2 is sulfided with 10 % H_2S–H_2, and sulfided TiO_2 acts as the promoter for Mo-based HDS catalyst[62]. Furthermore, sulfided TiO_2 is involved in the active phase of the HDS reaction[61]. The TPR profile of the TiO_2 support includes a small H_2 consumption

Table 1 The HDS Activities and CO Uptakes of the Rh–1.5P/MO_x Catalysts[56]

Support	Reduction temperature [℃]	HDS conversion [%]	CO uptake [μmol g^{-1}]	TOF[a] [h^{-1}]
SiO_2	550	55.0	71.7	202
TiO_2	650	54.6	18.6	777
Al_2O_3	800	54.6	52.9	271
ZrO_2	750	22.5	9.8	604
MgO	650	25.7	47.5	143

a) Calculated from CO uptake (assumed CO/Rh = 1).

peak at 550 ℃ for TiO_2[55], indicating that reduced TiO_2 (TiO_x) is formed above 550 ℃. TiO_x may react with H_2S to form sulfided TiO_2 (TiO_xS_y) in the HDS reaction. Therefore, the Rh–1.5P/TiO_2 catalyst showed the highest HDS activity at higher reduction temperature (600 ℃), and TiO_xS_y also acts as promoter and/or active site to enhance the TOF of Rh–P catalyst. We previously reported that the lower TOFs of NM–P catalysts can be explained by the presence of smaller noble metal phosphide particles[57]. Consequently, the high TOF of Rh–1.5P/ZrO_2 catalyst can be explained by the remarkably low CO uptake compared with other catalysts (**Table 1**). Regardless of the similar CO uptake, the TOFs were higher for Rh–1.5P catalyst supported on Al_2O_3 and SiO_2 than for catalysts supported on MgO, because the basic properties of MgO would lead to low sulfur tolerance of the Rh_2P catalyst.

3. Effect of P/NM Ratio on Formation and Hydrodesulfurization Activities of Noble Metal Phosphide Catalysts

3. 1. Nickel Phosphide

The effects of P loading on the formation of the nickel phosphide phase and on the HDS activity are well known[3),17)~19),23),24)]. Lower P/Ni ratio promotes the formation of $Ni_{12}P_5$ phase, which is an intermediate in the formation of Ni_2P[25]. In general, the Ni_2P phase has higher HDS activity than the $Ni_{12}P_5$ phase[18),21),23),24)]. Furthermore, Ni_2P catalyst has higher activity than Ni_5P_4 and NiP_2 among high P/Ni ratio catalysts[22]. Therefore, the P/Ni ratio is an important factor to determine the formation of the nickel phosphide phase and its HDS activity. Furthermore, reduction of the P precursor, in which the P/Ni ratio is higher than the stoichiometric ratio of Ni_2P (P/Ni = 0.5), results in the formation of the Ni_2P phase[17),18),24)]. Therefore, the optimal P/Ni ratio for high HDS activity of the Ni_2P catalyst is 0.8-2.2. As with the Ni_2P catalysts, the P/NM ratio should also strongly affect the formation of noble metal phosphide and its HDS activity.

3. 2. Rhodium Phosphide[54),58)]

Rh_2P catalyst on SiO_2, TiO_2, and Al_2O_3 supports showed superior HDS activities compared with MgO and ZrO_2 supports, as shown in **Table 1**. However, the formation of Rh_2P on Al_2O_3 requires higher reduction temperature due to the formation of $AlPO_4$, and the TOF of Rh_2P is remarkably enhanced by TiO_2 support[55]. Therefore, SiO_2, which has no strong interaction with Rh_2P or phosphate, is the superior support for clarifying the effects of P loading on Rh_2P formation and the catalytic activity for HDS reaction. Consequently, the effects of reduction temperature and P/NM ratio were examined on the formation of noble metal phosphide and on the HDS activities of NM–P/SiO_2 catalysts.

The catalysts were labeled as Rh–*x*P, where "*x*" denotes the P loading (wt%). The P/Rh ratio in the catalysts with 0.8, 1.5, 2.2 and 3.0 wt% P loading was 0.5, 1.0, 1.5 and 2.0, respectively. TPR and XRD analysis revealed that Rh_2P is easily formed in Rh–*x*P catalysts with higher P/Rh ratio[58]. Furthermore, RhP_2 was formed in the Rh–3.0P catalyst (P/Rh = 2.0) reduced at 650 ℃, but not in other catalysts[58]. However, transmission electron microscopy (TEM) and CO adsorption experiments revealed that the particle size of Rh_2P increased with P/Rh ratio[58]. The Rh–1.5P catalyst (P/Rh = 1.0) showed the highest HDS activity, which was four times greater than that of the Rh catalyst[58]. Thus, we concluded that moderate P loading (P/Rh = 1.0), which resulted in good reducibility of the phosphates and small Rh_2P particle size, resulted in the high HDS activity of the Rh–1.5P catalyst[58].

The catalytic stability was evaluated as relative activity (A/A_0), where A is the activity at any reaction time and A_0 is the initial activity (at 10 min)[54]. **Figure 2** shows the A/A_0 of reduced Rh–1.5P/SiO_2 and sulfided CoMoP/Al_2O_3 catalysts. After reaction for 1 h, the A/A_0 of CoMoP/Al_2O_3 catalyst remarkably decreased then remained stable from 5 h until 30 h. On the other hand, the A/A_0 of Rh–1.5P catalyst slightly decreased with time on stream, but remained higher than that of pre-sulfided CoMoP/Al_2O_3 catalyst at reaction time. Therefore, the Rh–1.5P/SiO_2 catalyst has higher stability and potential for HDS reaction than the commercial CoMoP/Al_2O_3 catalyst. Furthermore, the HDS activity of Rh–1.5P/SiO_2 catalyst was higher than that of Ni_2P/SiO_2 catalyst[54]. Rh_2P/SiO_2 catalyst also showed excellent stable activity for HDS of dibenzothiophene which was higher than that of Ni_2P/SiO_2 catalyst[71]. In

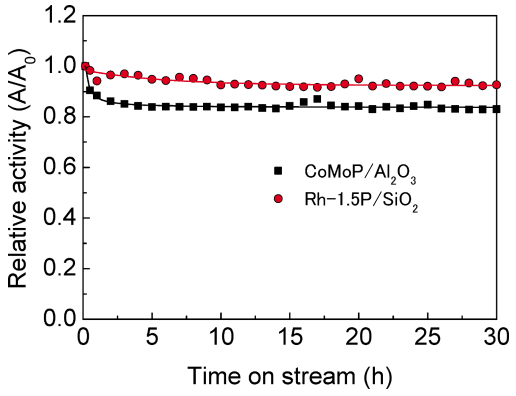

Pretreatment: $Rh–1.5P/SiO_2$ was reduced at 550 ℃ with H_2, $CoMoP/Al_2O_3$ was pre-sulfided at 400 ℃ with 5 vol% $H_2S–H_2$. Reaction conditions of thiophene HDS were $W/F = 37.9$ g h mol^{-1}, reaction temperature 350 ℃ and $H_2/C_4H_4S = 30$.

Fig. 2 Relative Activities (A/A_0) of $Rh–1.5P/SiO_2$ and $CoMoP/Al_2O_3$ Catalysts

addition, P in Rh_2P increases the sulfur tolerance of Rh[71].

3. 3. Palladium Phosphide

XRD demonstrated the peaks of PdO in $Pd–xP/SiO_2$ catalysts after calcination, as shown in **Fig. 3**. The TPR profiles of $Pd–xP/SiO_2$ catalysts are shown in **Fig. 4**. A negative peak appeared around 80 ℃, which was assigned to decomposition of palladium hydride[72], which is formed at room temperature. This peak temperature hardly changed with higher P/Pd ratio. Reduction of phosphate was observed above 600 ℃ in Pd–0.8P catalyst (P/Pd = 0.5). On the other hand, the reduction peak appeared around 350 ℃ in the TPR profiles of Pd–*x*P catalysts with higher P/Pd ratio (above 1.0). The reduction peak of nickel phosphate was observed in the TPR of Ni_2P/SiO_2 catalyst with a higher P/Ni ratio (above 1)[18]. The large peak at 350-400 ℃ in the TPR profiles of Rh–*x*P catalysts with higher P loadings (P/Pd ≥ 1.5) can be attributed to the reduction of rhodium phosphate[58]. These findings suggest that the peak observed at 350 ℃ could be attributed to the reduction of palladium phosphate.

The XRD patterns of Pd–*x*P catalysts reduced at 450-650 ℃ are shown in **Fig. 3**. Only the peaks for metallic Pd were observed in the patterns of Pd catalysts reduced at any temperature. A strong peak appeared around 40°, which contains the main peak of Pd and Pd_6P, and small Pd and Pd_6P peaks appeared for the Pd–0.8P catalyst (P/Pd = 0.5) reduced at 450 ℃. However, the Pd_3P peaks also appeared for this catalyst reduced above 550 ℃. These findings indicate that Pd_6P is an intermediate in the formation of Pd_3P. We previously reported that broad peaks for $Pd_{4.8}P$ were observed in the XRD patterns of Pd–1.5P catalyst (P/Pd = 1.0)[54]. However, other palladium phosphides (Pd_6P and Pd_3P) were also present in this catalyst. After reduction at 600 ℃, the Pd_3P phase was obtained from $NH_4H_2PO_2$ precursor (P/Pd = 1.2)[73]. On the other hand, the peaks for Pd_6P, $Pd_{4.8}P$ and Pd_3P were observed in the XRD pattern of the Pd–1.5P catalyst (P/Pd = 1.0) reduced at 550 ℃. These findings indicate that phosphate, which is difficult to reduce compared with hypophosphite, would induce formation of the more Pd rich phosphide. At higher P/Pd ratio, some palladium phosphides, such as Pd_6P, $Pd_{4.8}P$ and Pd_3P, were formed at lower reduction temperature (450 ℃). Furthermore, the broad peaks for Pd_5P_2 were observed in the Pd–*x*P catalysts with higher P/Pd ratio (above 1.0) reduced at 650 ℃. This phenomenon could be explained by the formation of disordered phosphides. On the basis of the TPR and XRD findings, palladium phosphides are easily formed at higher P/Pd ratio, as well as rhodium phosphide[58].

Figure 5 shows the effect of reduction temperature on the rate constant of the HDS reaction (k_{HDS}, assuming pseudo-first-order reaction) over the Pd–*x*P catalysts. The HDS activity of Pd catalyst slightly decreased with higher reduction temperature. In contrast, the optimal reduction temperatures for the maximum HDS activities of the Pd–*x*P catalysts were clearly observed. The optimal reduction temperature for the maximum HDS activity of the Pd–*x*P catalyst decreased with higher P/Pd ratio, indicating that the reducibility of phosphate and formation of phosphides strongly affect the HDS activity of Pd–*x*P catalyst. This trend was also observed in the Rh–*x*P catalysts[58]. **Table 2** shows the k_{HDS} and CO uptake of NM–*x*P catalysts. The highest k_{HDS} was obtained at P/Pd of 0.5. On the other hand, the CO uptake of the Pd–0.8P catalyst (P/Pd = 0.5) was the lowest among the Pd–*x*P catalysts, possibly because the high reduction temperature (650 ℃) caused aggregation of palladium phosphide.

3. 4. Ruthenium Phosphide

XRD revealed that RuO_2 was formed in all Ru–*x*P catalysts after calcination (**Fig. 6**). A small Ru peak appeared in the XRD patterns of Ru–*x*P catalysts with P/Ru ratio above 1.5. This trend was the same as that for the Rh–*x*P catalysts[58]. **Figure 7** shows the TPR profiles of Ru–*x*P catalysts. The peaks for reduction of RuO_2 appeared at 112 ℃ and 138 ℃ in the Ru catalyst, and shifted to higher temperatures with increasing P/Ru ratio. The same trend was observed in the TPR profiles of the Ni–P[18,23] and Rh–P[58] catalysts. These findings suggest that phosphate cover the RuO_2 particles, resulting in decreased reducibility of RuO_2. In contrast, the reduction peaks of phosphates shifted to lower temperature with increasing P/Ru ratio, as for the Rh–*x*P[58] and Pd–*x*P catalysts. However, the peaks from 300 to 600 ℃, which are assigned to reduction of phosphates interacting with noble metal and/or noble metal phosphates, did not appear for the Ru–1.5P catalyst (P/Ru = 1.0). On the other hand, the peaks from

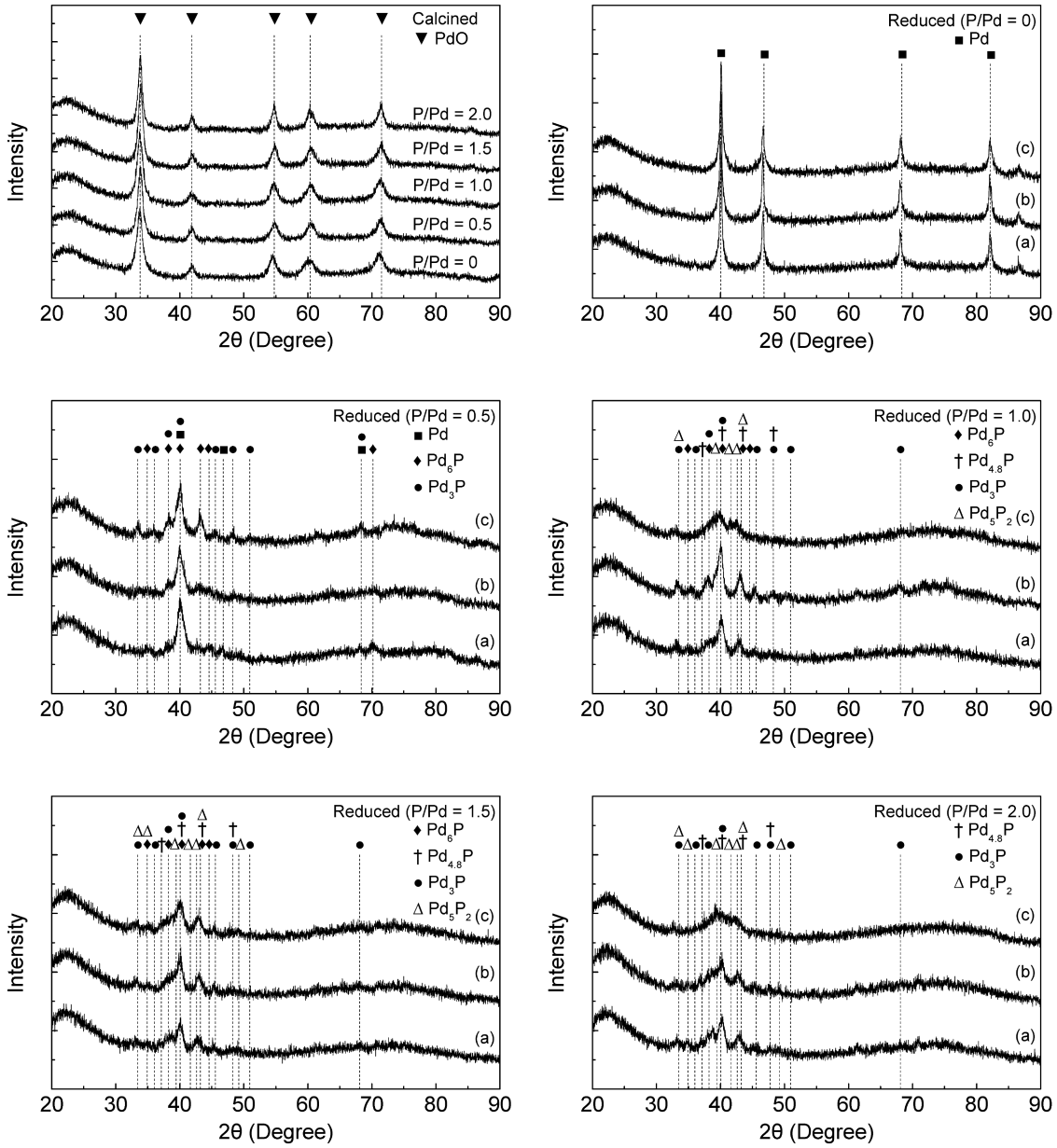

Reduction temperature: (a) 450 ℃, (b) 550 ℃, and (c) 650 ℃.

Fig. 3 XRD Patterns of Pd–xP/SiO_2 Catalysts after Calcination and Reduction

300 to 600 ℃ were clearly observed for the Rh–xP[58] and Pd–xP (**Fig. 4**) catalysts with the same P/NM ratio (1.0).

The formation of ruthenium phosphides was confirmed by XRD of the reduced Ru–xP catalysts (**Fig. 6**). Ru_2P was formed in the Ru–0.8P catalyst (P/Ru = 0.5) reduced at higher temperature (650 ℃), but metallic Ru also remained. Peaks for P rich ruthenium phosphide (RuP) were observed with P/Ru ratio above 1.5. These findings indicate that the reduction temperature and P/Ru ratio strongly affect the formation of ruthenium phosphides, as for rhodium and palladium phosphides. After reduction at 500 ℃, phase-pure Ru_2P catalyst was prepared from the precursor using $NH_4H_2PO_2$ with P/Ru ratio of 0.6[73]. In our study, since a small Ru peak ($2\theta = 44.1°$) was detected by XRD of Ru–P catalyst with P/Ru of 1.0 reduced at 650 ℃, phase-pure Ru_2P was not obtained, possibly because phosphate was used as a P precursor, which is harder to reduce than hypophosphite, as mentioned above.

Figure 8 shows the relationship between reduction temperature and HDS activities of Ru–xP catalysts. The maximum HDS activities of Ru–xP catalysts were obtained at around formation temperature of ruthenium phosphides. The trends for the Ru–xP catalysts were the same as those for the Rh–xP[58] and Pd–xP catalysts. The k_{HDS} and CO uptake of Ru–xP catalysts are listed in

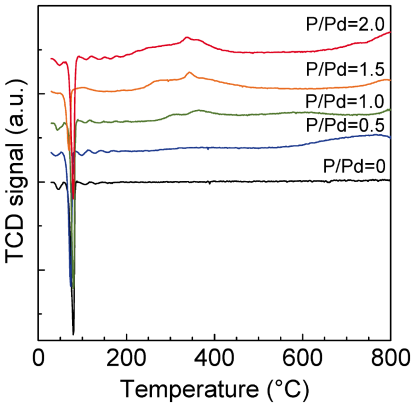

Fig. 4 TPR Profiles of Pd–xP/SiO_2 Catalysts

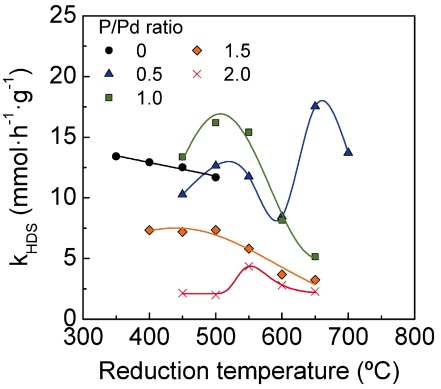

Fig. 5 Effect of Reduction Temperature on HDS Activities of Pd–xP/SiO_2 Catalysts

Table 2 HDS Activities and CO Uptakes of NM–xP/SiO_2 Catalysts

Catalyst	P loading [wt%]	P/NM	Reduction temperature [℃]	HDS rate [k_{HDS}, mmol h^{-1} g^{-1}]	CO uptake [μmol g^{-1}]
Pd–xP	0	0	350	13.4	51.4
	0.8	0.5	650	17.5	22.6
	1.5	1.0	500	16.2	31.2
	2.2	1.5	500	7.4	27.5
	3.0	2.0	550	4.4	23.9
Ru–xP	0	0	350	<0.1	11.0
	0.8	0.5	700	2.1	21.6
	1.5	1.0	650	3.6	16.3
	2.2	1.5	500	3.0	25.6
	3.0	2.0	450	1.6	43.1
Pt–xP	0	0	400	6.6	25.5
	0.8	1.0	450	2.8	9.2
	1.5	2.0	500	1.9	3.1
	2.2	3.0	450	1.4	2.1
	3.0	4.0	450	1.2	1.8

Table 2. Ru–1.5P catalyst (P/Ru = 1.0) showed the highest k_{HDS} among Ru–xP catalysts, and about 50 times greater than that of Ru catalyst. Supported Ru_2P and RuP catalysts exhibited higher HDS activities than supported Ru catalyst[74]. Calcination at higher temperature induce migration of RuO_2 leading to sintering on SiO_2 support[75),76]. The calcination temperature of NM–xP catalysts was 500 ℃, which is adequate for sintering of RuO_2 particles. However, the CO uptake of Ru–xP catalyst increased with higher P/Ru ratio. XRD of Ru–xP catalysts after calcination (**Fig. 6**) revealed that the intensity of RuO_2 peaks remarkably decreased and the width broadened with higher P/Ru ratio. Furthermore, shifts of the reduction peaks for RuO_2 were observed in the TPR profiles of Ru–xP catalysts, as shown in **Fig. 7**. The excess phosphates may interact with RuO_2 and inhibit the sintering caused in the calcination step at 500 ℃. Therefore, higher P/Ru ratio leads to increased CO uptake of Ru–xP catalyst.

3. 5. Platinum Phosphide

The range of P loading was the same for the Pt catalyst as for other NM–xP catalysts (0-3.0 wt%). However, the atomic weight of Pt is approximately twice that of other NMs (Rh, Pd, and Ru). Therefore, the range of P/Pt ratio is from 0 to 4.0.

Figure 9 shows the XRD patterns of calcined Pt–xP catalysts. Metallic Pt peaks were clearly observed instead of oxides in all catalysts. The TPR profiles of Pt–xP catalysts are shown in **Fig. 10**. No peaks indicating reduction of platinum oxides were found. Above 600 ℃, H_2 consumption, which was assigned to the reduction of phosphates on SiO_2 support[57),58)], was observed in the catalyst with P/Pt ratio of 1.0. The start of this H_2 consumption moved to lower temperature with higher P/Pt ratio. However, the peak temperature was little changed, indicating that phosphates strongly interact with SiO_2, but not Pt.

The XRD patterns of reduced Pt–xP catalysts are shown in **Fig. 9**. Unknown and PtP_2 peaks were observed with higher reduction temperature and P/Pt ratio. On the other hand, the peaks for metallic Pt appeared in the XRD patterns of Pt–3.0P catalyst (P/Pt = 4.0) reduced at 450 ℃ and 550 ℃ despite the higher P/Pt ratio. This finding indicates that Pt is less reactive

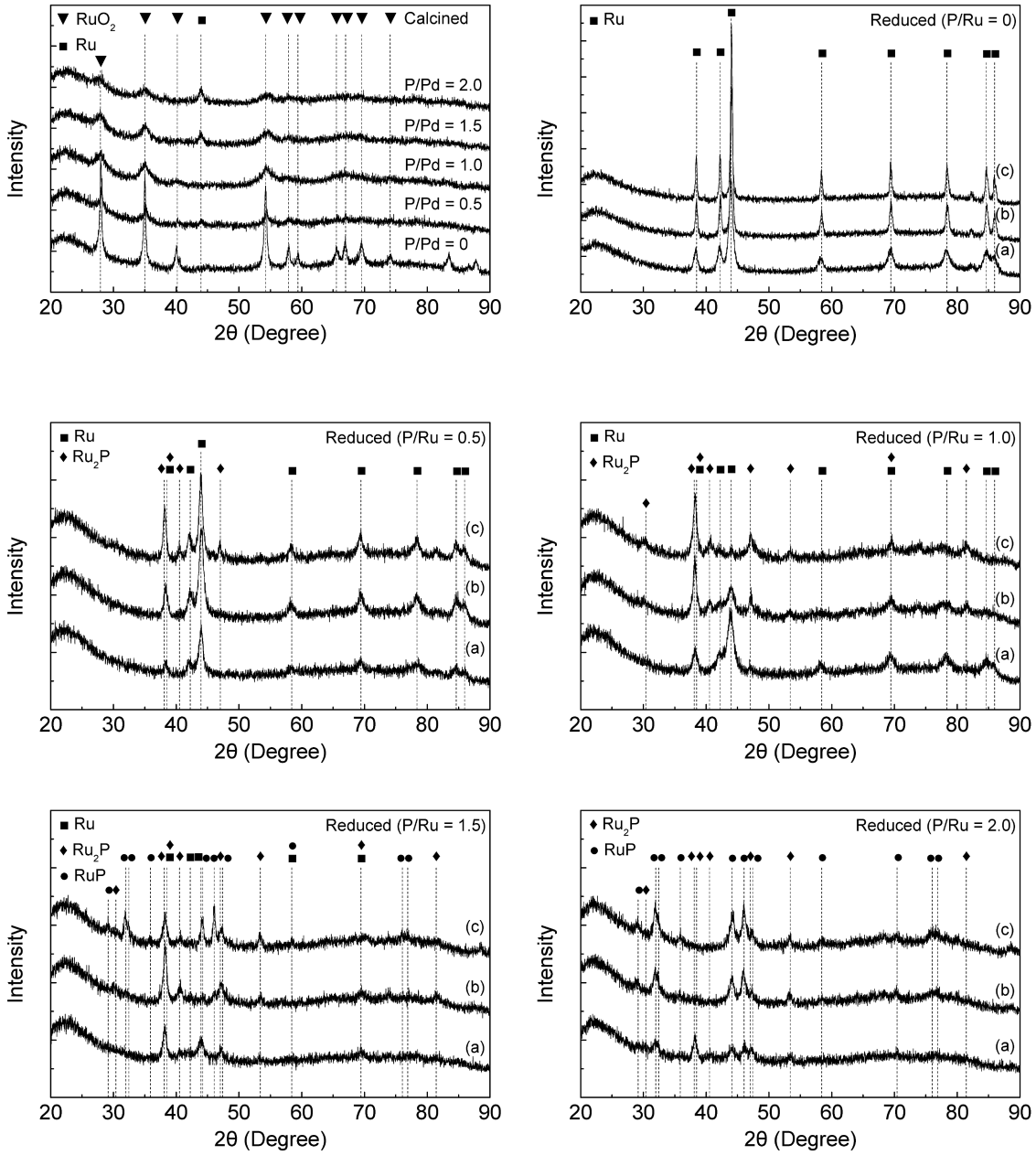

Reduction temperature: (a) 450 ℃, (b) 550 ℃, and (c) 650 ℃.

Fig. 6 XRD Patterns of Ru–xP/SiO_2 Catalysts after Calcination and Reduction

with P compared with other NMs. PtP_2 was formed in the Pt–xP catalyst reduced at 650 ℃ at P/Pt over 1.0. In other NM–xP catalysts, P loading excess to the stoichiometric z/y ratio resulted in the formation of noble metal phosphide (NM_yP_z).

The effect of reduction temperature on HDS activities of Pt–xP catalysts is shown in **Fig. 11**. The HDS activity of Pt catalyst decreased with higher reduction temperature. The HDS activities of the Pt–xP catalysts, except Pt–1.5P catalyst (P/Pt = 2.0), also decreased with higher reduction temperature.

Table 2 shows the k_{HDS} and CO uptake of Pt–xP catalysts. The k_{HDS} and CO uptake decreased with higher P/Pt ratio.

3. 6. Relationship between P/NM Ratio and HDS Activities of Noble Metal Phosphides

As mentioned above, the HDS activity of NM–xP catalyst was enhanced by the formation of noble metal phosphide. The optimal P/NM ratio for the maximum HDS activities of NM–xP catalysts depended on the type of NM, as shown in **Table 2**. Since metal rich phosphides (Pd_6P, $Pd_{4.8}P$ and Pd_3P), which have lower P/NM ratio than Rh_2P and Ru_2P, were formed in the Pd–xP catalysts (**Fig. 3**), the maximum HDS activity

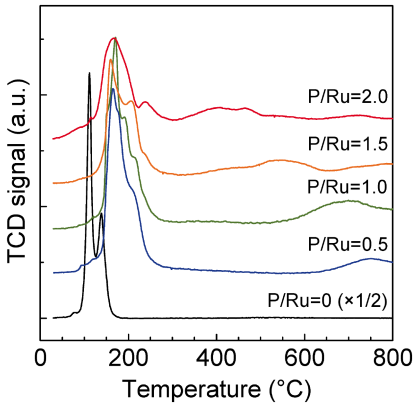

Fig. 7 TPR Profiles of Ru–xP/SiO_2 Catalysts

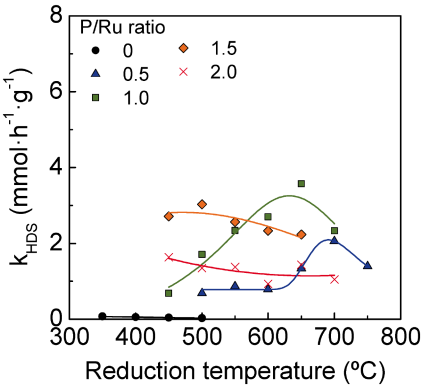

Fig. 8 Effect of Reduction Temperature on HDS Activities of Ru–xP/SiO_2 Catalysts

was obtained at lower P/NM ratio (0.5) for the Pd–xP catalyst than for the Rh–xP and Ru–xP catalysts (1.0). On the other hand, the HDS activity of NM–xP catalyst decreased with higher P/NM ratio above the optimal value.

In our previous study, CO uptake and TEM observations revealed that excess P caused aggregation of Rh_2P particles[58]. In this study, CO uptake of the Pd–xP catalyst also decreased with higher P/Pd ratio. Aggregation of palladium phosphide particle caused decrease of HDS activity at higher P/Pd ratio. However, the XRD patterns and CO uptake of Ru–xP catalysts indicated that excess P inhibits sintering of Ru species in the calcination step. Moreover, the average particle size of Ru–1.5P catalyst (11.5 nm, after reduction at 600 ℃) calculated from the TEM images was smaller than that of Ru catalyst (14.6 nm, after reduction at 450 ℃)[56]. Ni_2P catalyst showed higher activity than Ni_5P_4 and NiP_2 catalysts with high P/Ni ratio[22]. P rich ruthenium phosphide (RuP) was formed in the Ru–xP catalysts with higher P/Ru ratio, as shown in **Fig. 6**. Therefore, the low HDS activities of Ru–xP catalysts with higher P/Ru ratio (above 1.5) are probably caused by the formation of RuP.

The TPR and XRD findings showed that phosphates were less reactive with Pt in the Pt–xP catalyst. In addition, the HDS activity of Pt catalyst decreased with higher P/Pt ratio despite the formation of platinum phosphide, as shown in **Table 2**. Therefore, the decrease in HDS activity can be explained by the P covering the Pt sites[54] and/or low activity of platinum phosphide, such as PtP_2.

4. Hydrodenitrogenation Activities of Noble Metal Phosphide Catalysts[56]

In the NM–xP catalysts, except Pt–xP, high HDS activity was obtained with P/NM ratio of 1.0. Thus, the effects of reduction temperature on catalytic activities of NM and NM–1.5P for HDN of pyrrole (C_4H_4NH) were examined (**Fig. 12**). The HDN activities of Rh and Pd catalysts were little changed with higher reduction temperature. On the other hand, the HDN activity of Ru catalyst gradually decreased with increased reduction temperature from 450 to 600 ℃. Additionally, remarkably low HDN activity was observed at 650 ℃. The optimal reduction temperature for maximum HDN activity of the Pt catalyst was 400 ℃. The order of maximum HDN activities of the NM catalysts was Rh–Ru＞Pt＞Pd.

The HDN activity of Rh–1.5P catalyst decreased with higher reduction temperature. In contrast, optimal reduction temperatures for the maximum HDN activities of the Ru–1.5P[56] and Pd–1.5P catalysts were observed. The HDN activity of Pt–1.5P catalyst little changed with higher reduction temperature. The order of maximum HDN activities of the NM–1.5P catalysts was Rh–P＞Ru–P＞Pd–P＞Pt–P.

Since the aromatic C–N bond is stronger than the aliphatic C–N bond[45], the removal of the nitrogen atom is carried out through hydrogenation of the aromatic structure and breaking of the resulting aliphatic C–N bond[28),45),46]. Thus, NiMo and NiW catalysts, which have higher hydrogenation activity than CoMo catalyst, are often used for the HDN reaction[45]. We used $NiMoP/Al_2O_3$ as a reference catalyst to evaluate the HDN activities of NM–P catalysts. The HDN activity of sulfided $NiMoP/Al_2O_3$ catalyst (HDN conversion: 12.2 %)[56] was slightly lower than the maximum HDN activity of Pd–P catalyst (reduced at 600 ℃), indicating that Rh–P and Ru–P catalysts showed remarkably high HDN activity.

5. Conclusion

In the last decade of the 20th century, metal phosphide has been developed as a hydrotreating catalyst. Here we reported the preparation and catalytic performance of noble metal phosphides for hydrotreating reactions. The formation temperatures of Rh_2P on SiO_2

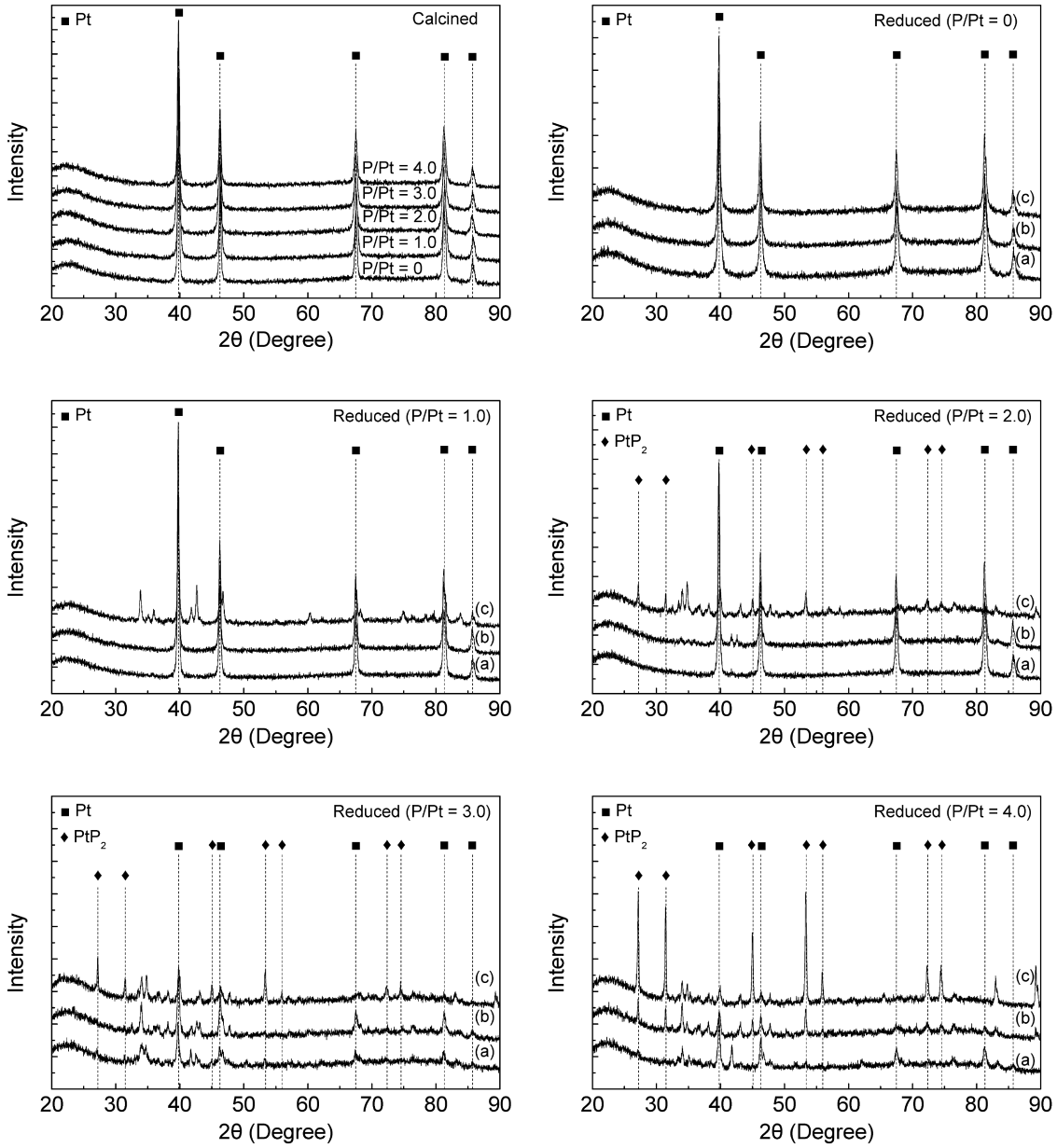

Reduction temperature: (a) 450 ℃, (b) 550 ℃, and (c) 650 ℃.

Fig. 9 XRD Patterns of Pt–xP/SiO_2 Catalysts after Calcination and Reduction

and TiO_2 supports were lower than those of other MO_x supports. In particular, the Al_2O_3 and ZrO_2 supports strongly interact with phosphate to form aluminum and zirconium phosphates, and these substances inhibit the formation of Rh_2P. Rh_2P catalyst supported on SiO_2, TiO_2 and Al_2O_3 showed high HDS activities. However, these maximum HDS activities were obtained at distinct reduction temperatures, indicating that Rh_2P formation strongly affects the HDS activity of Rh–P/MO_x catalyst. Formation of noble metal phosphides and HDS activities were influenced by the types of NM and P/NM ratio. The excess P interacts with NMs, except Pt, and formation of these species are important to form noble metal phosphides at lower reduction temperatures. Simultaneously, excess P causes negative effects, such as aggregation of noble metal phosphides (except Ru) and formation of P rich noble metal phosphides. Consequently, an optimal P/NM ratio for the maximum HDS activity of the NM–xP catalyst is observed. Rh–1.5P catalyst has high stability for HDS activity and remarkable high HDN activity. Therefore, Rh_2P has great potential as a new hydrotreating catalyst.

Acknowledgment

This work was supported in part by Grant-in-Aid for

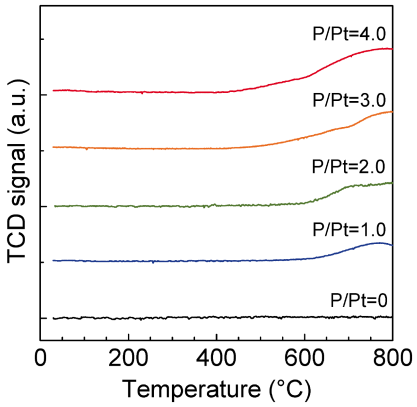

Fig. 10 TPR Profiles of Pt–xP/SiO_2 Catalysts

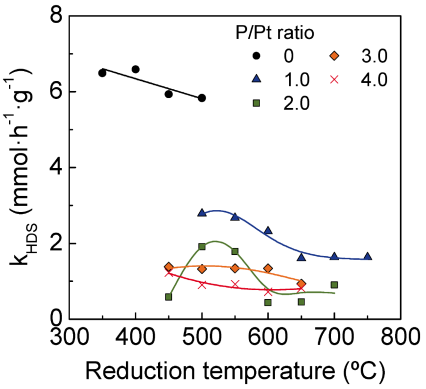

Fig. 11 Effect of Reduction Temperature on HDS Activities of Pt–xP/SiO_2 Catalysts

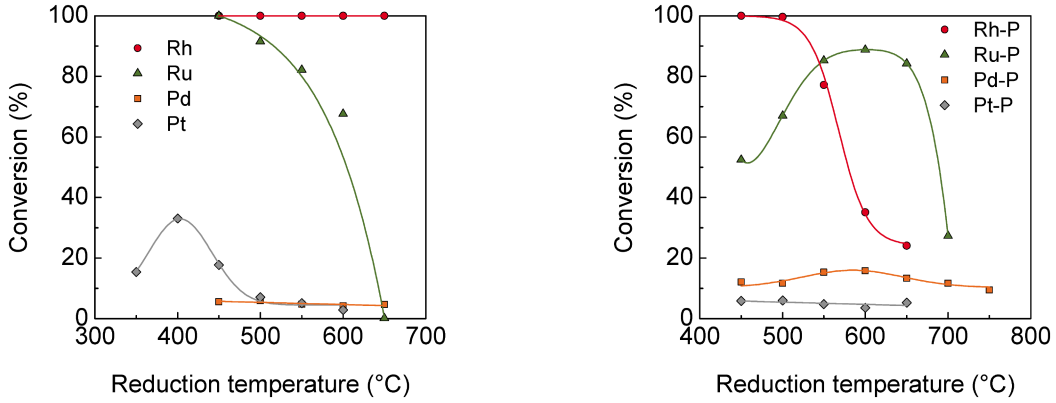

Reaction conditions of pyrrole HDN were $W/F = 652$ g h mol^{-1}, reaction temperature 320 ℃ and $H_2/C_4H_4NH = 523$.

Fig. 12 Effect of Reduction Temperature on HDN Activities of SiO_2-supported NM and NM−1.5P Catalysts

Young Scientists (B), Japan (21750158). The authors would like to thank Nippon Aerosil Co., Ltd., for supplying the SiO_2, TiO_2 and Al_2O_3 supports.

References

1) Okamoto, Y., *Catal. Today*, **132**, 9 (2008).
2) Oyama, S. T., Gott, T., Zhao, H., Lee, Y. K., *Catal. Today*, **143**, 94 (2009).
3) Prins, R., Bussell, M. E., *Catal. Lett.*, **142**, 1413 (2012).
4) Okamoto, Y., *Bull. Chem. Soc. Jpn.*, **87**, (1), 2058 (2014).
5) Topsøe, H., Clausen, B. S., Candia, R., Wivel, C., Mørup, S., *J. Catal.*, **68**, 433 (1981).
6) Fujikawa, T., *Catal. Surv. Asia*, **10**, 89 (2006).
7) Usman, Yamamoto, T., Kubota, T., Okamoto, Y., *Appl. Catal. A: General*, **328**, 219 (2007).
8) Shimizu, T., Hiroshima, K., Honma, T., Mochizuki, T., Yamada, M., *Catal. Today*, **45**, 271 (1998).
9) Sun, M., Nicosia, D., Prins, R., *Catal. Today*, **86**, 173 (2003).
10) Ramanathan, S., Oyama, S. T., *J. Phys. Chem.*, **99**, 16365 (1995).
11) Aegerter, P. A., Quigley, W. W. C., Simpson, G. J., Ziegler, D. D., Logan, J. W., McCrea, K. R., Glazier, S., Bussell, M. E., *J. Catal.*, **164**, 109 (1996).
12) Dhandapani, B., Clair, T. St., Oyama, S. T., *Appl. Catal. A: General*, **168**, 219 (1998).
13) Lewandowski, M., Szymańska-Kolasa, A., Da Costa, P., Sayag, C., *Catal. Today*, **119**, 31 (2007).
14) Liu, P., Rodriguez, J. A., Asakura, T., Gomes, J., Nakamura, K., *J. Phys. Chem. B*, **109**, 4575 (2005).
15) Nagai, M., *Appl. Catal. A: General*, **322**, 178 (2007).
16) Robinson, W. R. A. M., van Gestel, J. N. M., Koranyi, T. I., Eijsbouts, S., van der Kraan, A. M., van Veen, J. A. R., de Beer, V. H. J., *J. Catal.*, **161**, 539 (1996).
17) Stinner, C., Tang, Z., Haouas, M., Weber, Th., Prins, R., *J. Catal.*, **208**, 456 (2002).
18) Oyama, S. T., Wang, X., Lee, Y. K., Bando, K., Requejo, F. G., *J. Catal.*, **210**, 207 (2002).
19) Oyama, S. T., *J. Catal.*, **216**, 343 (2003).
20) Rodriguez, J. A., Kim, J. Y., Hanson, J. C., Sawhill, S. J., Bussell, M. E., *J. Phys. Chem. B*, **107**, 6276 (2003).
21) Sawhill, S. J., Philips, D. C., Bussell, M. E., *J. Catal.*, **215**, 208 (2003).
22) Korányi, T. I., *Appl. Catal. A: General*, **239**, 253 (2003).
23) Wang, A., Ruan, L., Teng, Y., Li, X., Lu, M., Rena, J., Wanga, Y., Hu, Y., *J. Catal.*, **229**, 314 (2005).
24) Sawhil, S. J., Layman, K. A., Van Wyk, D. R., Engelhard, M. H., Wang, C., Bussell, M. E., *J. Catal.*, **231**, 300 (2005).
25) Yang, S., Liang, C., Prins, R., *J. Catal.*, **237**, 118 (2006).
26) Yang, S., Liang, C., Prins, R., *J. Catal.*, **241**, 465 (2006).
27) Lee, Y. K., Oyama, S. T., *Appl. Catal. A: General*, **322**, 191 (2007).
28) Abu, I. I., Smith, K. J., *Catal. Today*, **125**, 248 (2007).

29) Oyama, S. T., Lee, Y. K., *J. Catal.*, **258**, 393 (2008).
30) Wang, R., Smith, K. J., *Appl. Catal. A: General*, **361**, 18 (2009).
31) da Silva, V. T., Sousa, L. A., Amorim, R. M., Andrini, L., Figueroa, S. J. A., Requejo, F. G., Vicentini, F. C., *J. Catal.*, **279**, 88 (2011).
32) Bando, K. K., Wada, T., Miyamoto, T., Miyazaki, K., Takakusagi, S., Koike, Y., Inada, Y., Nomura, M., Yamaguchi, A., Gott, T., Oyama, S. T., Asakura, K., *J. Catal.*, **286**, 165 (2012).
33) Savithra, G. H. L., Muthuswamy, E., Bowker, R. H., Carrillo, B. A., Bussell, M. E., Brock, S. L., *Chem. Mater.*, **25**, 825 (2013).
34) Carenco, S., Portehault, D., Boissière, C., Mézailles, N., Sanchez, C., *Chem. Rev.*, **113**, (10), 7981 (2013).
35) Clark, P., Li, W., Oyama, S. T., *J. Catal.*, **200**, 140 (2001).
36) Clark, P., Wang, X., Oyama, S. T., *J. Catal.*, **207**, 256 (2002).
37) Phillips, D. C., Sawhill, S. J., Self, R., Bussell, M. E., *J. Catal.*, **207**, 266 (2002).
38) Clark, P. A., Oyama, S. T., *J. Catal.*, **218**, 78 (2003).
39) Montesinos-Castellanos, A., Zepeda, T. A., Pawelec, B., Fierro, J. L. G., de los Reyes, J. A., *Chem. Mater.*, **19**, 5627 (2007).
40) Duan, X., Li, X., Wang, A., Teng, Y., Wang, Y., Hu, Y., *Catal. Today*, **149**, 11 (2010).
41) Segawa, K., Takahashi, K., Satoh, S., *Catal. Today*, **63**, 123 (2000).
42) Girgis, M. J., Gates, B. C., *Ind. Eng. Chem. Res.*, **30**, 2021 (1991).
43) Furimskya, E., Massoth, F. E., *Catal. Today*, **52**, 381 (1999).
44) Ho, T. C., *J. Catal.*, **219**, 442 (2003).
45) Mochida, I., Choi, K. H., *J. Jpn. Petrol. Inst.*, **47**, (3), 145 (2004).
46) Wang, H., Prins, R., *Catal. Lett.*, **126**, 1 (2008).
47) Kanda, Y., Uemichi, Y., Kobayashi, T., Andalaluna, L., Sugioka, M., *Stud. Surf. Sci. Catal.*, **156**, 747 (2005).
48) Kanda, Y., Kobayashi, T., Uemichi, Y., Sugioka, M., *J. Jpn. Petrol. Inst.*, **49**, (2), 49 (2006).
49) Kanda, Y., Kobayashi, T., Uemichi, Y., Namba, S., Sugioka, M., *Appl. Catal. A: General*, **308**, 111 (2006).
50) Kanda, Y., Ooka, Y., Kobayashi, T., Uemichi, Y., Sugioka, M., *J. Jpn. Petrol. Inst.*, **50**, (1), 61 (2007).
51) Kanda, Y., Aizawa, T., Kobayashi, T., Uemichi, Y., Namba, S., Sugioka, M., *Appl. Catal. B: Environmental*, **77**, 117 (2007).
52) Kanda, Y., Seino, A., Kobayashi, T., Uemichi, Y., Sugioka, M., *J. Jpn. Petrol. Inst.*, **52**, (2), 42 (2009).
53) Kanda, Y., Iwamoto, H., Kobayashi, T., Uemichi, Y., Sugioka, M., *Top. Catal.*, **52**, 765 (2009).
54) Kanda, Y., Temma, C., Nakata, K., Kobayashi, T., Sugioka, M., Uemichi, Y., *Appl. Catal. A: General*, **386**, 171 (2010).
55) Kanda, Y., Nakata, K., Temma, C., Sugioka, M., Uemichi, Y., *J. Jpn. Petrol. Inst.*, **55**, (2), 108 (2012).
56) Kanda, Y., Araki, T., Sugioka, M., Uemichi, Y., *J. Jpn. Petrol. Inst.*, **56**, (2), 94 (2013).
57) Kanda, Y., Ichiki, T., Kayaoka, S., Sawada, A., Sugioka, M., Uemichi, Y., *Chem. Lett.*, **42**, 404 (2013).
58) Kanda, Y., Temma, C., Sawada, A., Sugioka, M., Uemichi, Y., *Appl. Catal. A: General*, **457**, 410 (2014).
59) Sweeney, C. M., Stamm, K. L., Brock, S. L., *J. Alloys Comp.*, **448**, 122 (2008).
60) Damyanova, S., Spojakina, A., Jiratova, K., *Appl. Catal. A: General*, **125**, 257 (1995).
61) Wang, D., Qian, W., Ishihara, A., Kabe, T., *J. Catal.*, **203**, 322 (2001).
62) Coulier, L., van Veen, J. A. R., Niemantsverdriet, J. W., *Catal. Lett.*, **79**, 149 (2002).
63) Saih, Y., Nagata, M., Funamoto, T., Masuyama, Y., Segawa, K., *Appl. Catal. A: General*, **295**, 11 (2005).
64) Chen, J., Zhou, S., Ci, D., Zhang, J., Wang, R., Zhang, J., *Ind. Eng. Chem. Res.*, **48**, (8), 3812 (2009).
65) Yasuda, H., Sato, T., Yoshimura, Y., *Catal. Today*, **50**, 63 (1999).
66) Simon, L. J., Ommen, J. G. V., Jentys, A., Lecher, J. A., *Catal. Today*, **73**, 105 (2002).
67) Barrio, V. L., Arias, P. L., Cambra, J. F., Güemez, M. B., Pawelec, B., Fierro, J. L. G., *Catal. Commun.*, **5**, 173 (2004).
68) Tauster, S. J., *Acc. Chem. Res.*, **20**, 389 (1987).
69) Bernal, S., Calvino, J. J., Cauqui, M. A., Gatica, J. M., López Cartes, C., Pérez Omil, J. A., Pintado, J. M., *Catal. Today*, **77**, 385 (2003).
70) Ruckenstein, E., Wang, H. Y., *J. Catal.*, **187**, 151 (1999).
71) Hayes, J. R., Bowker, R. H., Gaudette, A. F., Smith, M. C., Moak, C. E., Nam, C. Y., Pratum, T. K., Bussell, M. E., *J. Catal.*, **276**, 249 (2010).
72) Lieltza, G., Nimza, M., Völtera, J., Läzärb, K., Guczib, L., *Appl. Catal.*, **45**, 71 (1988).
73) Bowker, R. H., Smith, M. C., Carrillo, B. A., Bussell, M. E., *Top. Catal.*, **55**, 999 (2012).
74) Guan, Q., Sun, C., Li, R., Li, W., *Catal. Commun.*, **14**, 114 (2011).
75) Lopez, T., Bosch, P., Asomoza, M., Gomez, R., *J. Catal.*, **133**, 247 (1992).
76) Reyes, P., König, M. E., Pecchi, G., Concha, I., López Granados, M., Fierro, J. L. G., *Catal. Lett.*, **46**, 71 (1997).

.....

要　　旨

新規水素化処理触媒としての貴金属リン化物 —高活性リン化ロジウム触媒—

神田　康晴，上道　芳夫

室蘭工業大学大学院工学研究科くらし環境系領域，050-8585 北海道室蘭市水元町27-1

新たな水素化処理触媒として金属リン化物が注目されている。著者らは新たなリン化物系水素化処理触媒を開発するため，貴金属リン化物の調製とその触媒特性について検討した。担体はリン前駆体であるリン酸の還元性に強く影響を与えるため，Rh_2P の生成温度は用いる担体により異なった。特に，リン酸との相互作用の弱い SiO_2 および TiO_2 担体上では他の担体よりも Rh_2P が低温で生成した。また，Rh_2P の生成に伴い，Rh–P/MO_x 触媒の HDS 活性が向上することを明らかにした。さらに，貴金属（NM）の種類および P/NM 比は貴金属リン化物の生成と HDS 活性に対して影響を与え，過剰な P を添加した触媒では貴金属リン化物が低温で生成するものの，凝集による粒子径の増大および P リッチなリン化物の生成を引き起こした。このため，P/NM 比が異なる NM–xP 触媒の HDS 活性には最適な P/NM 比が見られた。HDS 反応に対して Rh–1.5P 触媒は高く安定な活性を示した。加えて，この触媒の HDN 活性は硫化処理した NiMoP/Al_2O_3 触媒の活性よりも著しく高かった。したがって，Rh_2P は新たな水素化処理触媒として高い可能性を有していると判断される。

……